DESERT

Desert
Online at http://desert.ut.ac.ir

Desert 24-2 (2019) 331-353

# Tracing environmental changes and paleoclimate using the micromorphology of soils and desert varnish in central Iran

M. Sarmast[a], M.H. Farpoor[a*], A. Jafari[a], I. Esfandiarpour Borujeni[b]

[a] *Department of Soil Science, Faculty of Agriculture, Shahid Bahonar University of Kerman, Kerman, Iran*
[d] *Department of Soil Science, Faculty of Agriculture, Vali-e-Asr University of Rafsanjan, Rafsanjan,Kerman, Iran*

Received: 28 May 2019; Received in revised form: 8 October 2019; Accepted: 5 November 2019

**Abstract**

Soil and desert varnish are powerful records capable of saving invaluable data regarding environmental factors and processes during their formation stages. The present research was carried out to identify the environmental variations and paleoclimate reconstruction in the central deserts of Iran using soil and varnish micromorphological characteristics. Mantled pediment, alluvial fan, and alluvial plain landforms were selected. A minimum of one representative pedon was described and sampled on each geomorphic surface, amounting to a total of eight pedons. Varnished rocks were further collected from all geomorphic surfaces and studied by petrography microscope. Clay (coatings and micro layers), calcite (nodules, coatings, quasicoatings, and infillings), anhydrite (nodules), halite (coatings) pedofeatures, clay coating-calcite infilling, and anhydrite nodule-clay coating compound pedofeatures were investigated in the thin sections of the soil. Lenticular, vermiform, and platy gypsum crystals were identified as nodules and interlocked plates. Desert varnishes (100-600 µm) were different from host rocks as far as color, texture, and formative components are concerned. According to micromorphological evidence, the area probably experienced two different climates. Coatings and infillings of clay in soils and rock crevices were developed in an environment with more available humidity. Evaporite minerals were formed in soils and clay coatings on rock surfaces in the following period with less available moisture. The study results showed that micromorphology could be a necessary and useful tool in pedology and paleopedology investigations.

***Keywords:*** Clay pedofeatures; Evaporite minerals; Palaeopedology; Subaerial coating; Varnish microlamination

## 1. Introduction

Soil micromorphology is a useful tool for the description, interpretation, and measurement of features, components, and fabrics in soils and sediments (Bullock *et al*., 1985). Genesis, classification, and management of soils together with soil characterization in palaeopedology and archaeology are among the topics highlighted by micropedology (Stoops, 2010). Besides, micromorphological features along with other soil data provide crucial information for the reconstruction of the formation processes and paleoenvironmental conditions of buried and polygenetic modern soils and paleosols (Kemp, 2013).

As a wide depression between Alborz and Zagros Mountains, Central Iranian Plateau has experienced various geological events (Darvishzadeh, 1991). The plateau is located on the ancient bed of Tethys Ocean (Krinsley, 1970). Orogenic activities of late Cretaceous has cut off the plateau from the Tethys seaway (Sengör *et al*., 1988). The warming of the climate which commenced at the end of Paleocene, continued through to the Cenozoic era (Zachos *et al*., 1993), in turn augmenting the formation of inter-mountain continental basins. Jiroft area is an isolated basin in central Iran suitable for palepedology investigations.

Invaluable data on soil forming factors and processes, and (paleo) climate have been provided by soil micromorphology in Central Iranian Plateau (Ayoubi *et al*., 2006; Bayat *et al*., 2017; Khademi and Mermut, 2003; Khormali *et al*., 2003, 2006; Moazallahi and Farpoor, 2009).

* Corresponding author. Tel.: +98 34 31322656
Fax: +98 34 31322656
*E-mail address*: farpoor@uk.ac.ir

Presence of thick clay coatings in the paleoargillic horizons of soils in arid and semi-arid environments has been attributed to a climate with more available humidity in the past (Ayoubi *et al.*, 2006; Farpoor *et al*., 2012; Khademi and Mermut, 2003; Khormali *et al*., 2003). Meanwhile, clay illuviation and formation of clay coatings in such environments evidence the long time stability in the landscape (Gunal and Ransom, 2006; Khormali and Ajami, 2011; Khormali *et al*., 2003; Sarmast *et al*., 2017a). Moreover, climatic changes are mainly recorded by the fabric and composition of calcic (Durand *et al*., 2010), gypsic (Poch *et al*., 2010) or salic (Mees and Tursina, 2010) horizons. Therefore, micromorphology investigations are definitely conducive to understanding environmental changes and paleoclimate in arid and semi-arid areas (Stoops, 2010).

Desert varnish, among the most important archives of environmental changes in desert areas, has been used for paleoclimate reconstruction of desert landscapes (Liu, 2003; Liu and Broecker, 2013, 2008, 2007; Zerboni, 2008). It is defined as a type of rock cover (Dorn, 2013) composed of Fe and Mn oxides, phyllosilicate clay minerals, and trace and rare earth elements (Potter and Rossman, 1979, 1977; Thiagarajan and Lee, 2004). Continuous slow deposition of mineral grains over centuries has formed this cover on stable rock surfaces (Liu and Broecker, 2000). Desert varnish is made of components with external origin, mainly composed of dust and aerosols deposited from the atmosphere (Dorn *et al*., 2013; Goldsmith *et al*., 2014, 2012; Hodge *et al*., 2005; Thiagarajan and Lee, 2004). Accordingly, local and regional changes in dust, climatic fluctuations, and erosion and sedimentation processes could be reflected by use of desert varnish components (Watchman, 2000). Sedimentary origin of desert varnish causes microlamination, in turn a record of environmental change during formation (Perry and Adams, 1978).

Landforms in Jiroft area, central Iran, are covered by a thick continuous layer of desert pavements covered by a brown to black varnish. Physical and chemical properties of varnish in this area together with clay mineralogy were investigated in previous studies. Desert varnish in Jiroft area is composed of particles <0.2-50 µm with a cation exchange capacity range of 8.5–21 $cmol_c kg^{-1}$. Magnetic susceptibility in varnish samples was reported between 300 and 1855 $10^{-8}$ $m^3$ $kg^{-1}$, and Si, Ca, Al, Fe, and Mg concentrations were 26.4, 3.9, 3.8, 3.1, and 2.2%, respectively (Sarmast *et al*., 2017a). Additionally, age index (cation ratio) of desert varnish was used for landscape evolution in the area (Sarmast *et al*., 2017a).

The micromorphology of desert varnish formed on different geomorphic surfaces in the Jiroft area, central Iran, was investigated in the present research. The structure of desert varnish was studied through making micromorphology observations. Microlaminations were observed with a petrographic microscope after thin sections of varnish were polished to about 5-10 µm thick. The color of microlayers in varnish is controlled by environmental changes and could be utilized as an index in microscopic studies. Several researchers have shown that dark layers are enriched by Mn and formed under humid conditions while Fe, Al, and Si are characterized by yellow/orange layers formed during arid periods (Liu, 2003; Liu and Broecker, 2013, 2008, 2007; Liu and Dorn, 1996). Slow release and high oxidation rate of Mn in highly alkaline (arid) environments cause Fe enriched aeolian clay minerals to be concentrated in varnish, leading to a reduction in Mn/Fe ratio (Jones, 1991). On the other hand, the increase in soluble Mn in humid environments, provides ideal conditions for Mn accumulation in microlayers (dark) of the desert varnish, compared to Fe (Goldsmith *et al*., 2014; Thiagarajan and Lee, 2004).

Micromorphology has been extensively employed by myriad researchers to study the genesis and development of modern soils and paleosols, environmental change, and paleoclimate reconstruction. Furthermore, the microlamination of desert varnish, as a chronometric tool, has been considered in several studies. However, no research has performed a micromorphological characterization of desert varnish compared to underlain soil. Therefore, the present research focused on the characterization of environmental and climatic conditions during the formation and development of soil and desert varnish using micromorphological investigations in a desert landscape.

The main objectives of this research were as follows:

1) to study environmental conditions during the formation and development of soils and desert varnishes in a desert landscape using micromorpholgy; 2) to reconstruct climatic fluctuations in the same landscape from past to the present.

## 2. Materials and Methods

### 2.1. Study area

The study area is located in the south of Kerman Province, central Iran (Fig. 1). The climate of the area is semi-arid desertous with a mean annual rainfall of 140 mm and a mean annual temperature of 25 °C. Weak aridic and hyperthermic soil moisture and temperature regimes were investigated in this area, respectively (Van Wambeke, 1986). Soils of the area were not cultivated; they were dominantly covered by varnished desert pavement without considerable vegetation cover. From a geological perspective, the area under study is composed of igneous parent material (Babakhani *et al*., 1992). Sedimentary calcareous and gypsiferous evaporites are further distributed in the area (Fig. 1).

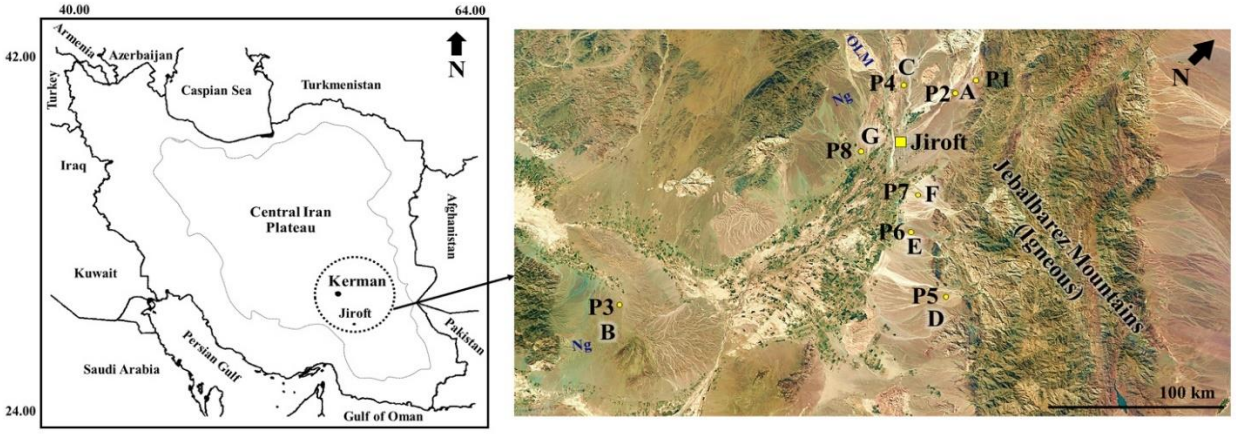


Fig. 1. Maps of the study area in central Iran and the studied geomorphic surfaces in Jiroft area. Dots indicate the location of pedons on different geomorphic surfaces. Abbreviations are calcareous marls (OLM) and gypsiferous marl (Ng). Seven geomorphic surfaces: stable surface of mantled pediment (A), north-south direction; semi-stable surface of mantled pediment (B), south-north direction; unstable surface of mantled pediment (C), north-south slope direction; apex of alluvial fan (D), east-west direction; stable surface of mid alluvial fan (E), east-west direction; unstable surface of mid alluvial fan (F), east-west direction; alluvial plain (G)

### 2.2. Studied landforms and geomorphic surfaces

For this research, we selected stable, semi-stable, and unstable surfaces of mantled pediment, apex of alluvial fan, stable and unstable surfaces of mid alluvial fan, and alluvial plain geomorphic surfaces (Fig. 1) based on soil formation history, soil type, stability and development of the landforms, and their relative age (Table 1, Fig. 2; Sarmast *et al*., 2017a, 2017b, 2016). The Central Iranian Plateau was once part of the PaleoTethys Ocean (Krinsley, 1970). The Tethys seaway was cut off by late Cretaceous to Miocene orogenic activities, forming shallow water bodies between the mountains (Sengör *et al.*, 1988). The study area seems to be one of those old shallow water bodies. Mantled pediments were formed by erosion and sedimentation accelerated by uplift in that era. Sedimentation of thick layers of coarse-textured alluvium in the eastern portion of study area formed alluvial fans. Upstream debris flows resulted in the deposition of detrital coarse sediments, causing the formation of apex surface in the early stages of alluvial fan formation. Alluvial fans were extended by continuous interfingering of debris flows with fine-sized stream sediments which formed the mid alluvial fan surface (Gutiérrez, 2005). Ultimately, Jiroft plain was formed by the evaporation of shallow saline intermountain water bodies due to the arid and warm environment of late Paleocene and its continuation in the Cenozoic (Zachos *et al*., 1993) (Sarmast *et al*., 2017a).

### 2.3. Field work

#### 2.3.1. Soil sampling

In each geomorphic surface with a total of eight pedons, at least one pedon was selected, described (Schoeneberger *et al.*, 2012), and sampled (Figs. 1, 2). Soil samples were air-dried, crushed, and passed through a 2 mm sieve for physicochemical analyses. Undisturbed soil samples were further collected from genetic horizons for micromorphological observations.

#### 2.3.2. Desert varnish sampling

About 50 rocks with dominant varnish of the area were collected from each studied geomorphic surface. Desert varnish only forms on the upward face of the rocks with no

displacement and movement during varnish formation (Fig. 3). Thus, the bottom, ground-facing side of rocks was analyzed to ensure that the rocks were not turned over. No signs of erosion or weathering were observed on the rock surfaces. Igneous rocks were the bedrock for almost all desert varnish samples. The selected rocks were primarily washed by distilled water and then by ethanol.

Table 1. Selected characteristics of the studied landforms and geomorphic surfaces

| Landform | Geomorphic surface | Pedons | Soil RSG[a] | Soil Taxonomy[b] | Soil $Fe_o/Fe_d$[c] | Varnish (Ca+K)/Ti[d] |
|---|---|---|---|---|---|---|
| Mantled pediment | Stable surface of mantled pediment | 1, 2 | Calcisols | Typic Calciargids | 0.03 | 6.14 |
| | Semi-stable surface of mantled pediment | 3 | Solonchaks | Anhydritic Haplosalids | 0.03 | 6.50 |
| | Unstable surface of mantled pediment | 4 | Gypsisols | Typic Calcigypsids | 0.05 | 7.66 |
| Alluvial fan | Apex of alluvial fan | 5 | Fluvisols | Typic Torrifluvents | 0.35 | 8 |
| | Stable surface of mid alluvial fan | 6 | Fluvisols | Typic Torrifluvents | 0.20 | 8.80 |
| | Unstable surface of mid alluvial fan | 7 | Fluvisols | Typic Torrifluvents | 0.20 | 9.75 |
| Alluvial plain | - | 8 | Solonchaks | Anhydritic Haplosalids | 0.03 | 14 |

[a] Reference soil group (IUSS Working Group WRB, 2015), data from Sarmast *et al*. (2016)
[b] Soil Survey Staff (2014)
[c, d] Data from Sarmast *et al.* (2017a)

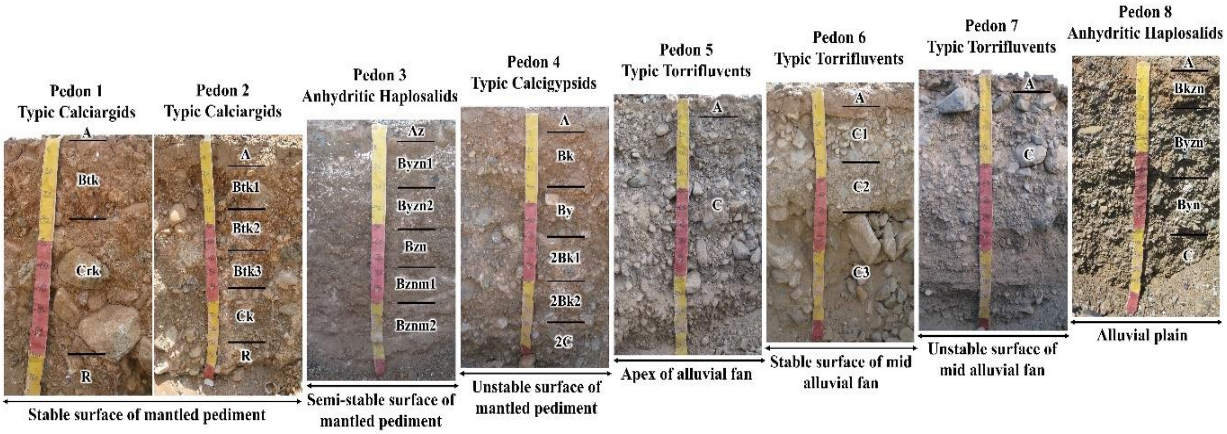


Fig. 2. Lithostratigraphy of the eight studied pedons.

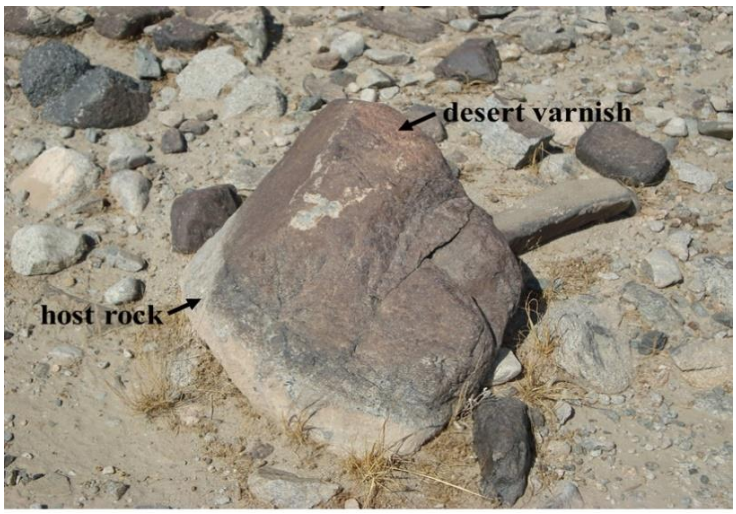


Fig. 3. Studied desert varnish on the top surface of the host rock

*2.4. Soil laboratory analyses*

Pipet method (Gee and Bauder, 1986) was used to examine the particle size distribution. The pH of saturated paste and the electrical conductivity (EC) of saturated extract were determined by Jenway pH and EC meters. Back titration (Nelson, 1982) was employed to specify the equivalent calcium carbonate. Aceton (Nelson, 1982) and oven (Artieda *et al*., 2006) methods were utilized for the investigation of gypsum+anhydrite and gypsum, respectively. Anhydrite content was calculated by the destruction of the above contents (Wilson *et al*., 2013). Soluble $Na^+$ and $K^+$, determined by flame photometry (Gammon, 1951), and soluble $Ca^{+2}$ and $Mg^{+2}$, investigated by complexometry (Ringbom *et al*., 1958) method, were the basis for the calculation of sodium adsorption ratio (SAR).

*2.5. Micromorphological studies*

Soil thin sections were provided using Murphy (1986) guideline. The method described by Liu and Dorn (1996) was considered to prepare the ultrathin sections from the rocks containing desert varnish. Sections were observed and photographed under plain and cross polarized lights by a BK-POL TD petrography microscope. Stoops (2003) guideline was utilized for soil thin section description.

## 3. Results and Discussions

*3.1. Soil macromorphological characteristics*

Table 2 shows the selected morphological, physical, and chemical properties of the studied soils.

Sequence of A, Btk, Ck, and R horizons was found in the Typic Calciargids of stable mantled pediment (Fig. 2). Carbonate masses and clay bodies (lamellae) were observed in argillic and calcic horizons and calcite pendants were detected in Ck horizon (Table 2). The current arid climate does not have enough humidity for the argillic horizon formation. Meanwhile, the SAR content is not high enough for clay dispersion and formation of Btk horizon in the arid climate of the area. Therefore, the formation of such morphological features could be attributed to climatic fluctuations during soil formation on a stable surface, forming polyphase soils (Farpoor and Irannejad, 2013; Khademi and Mermut, 2003; Khormali *et al*., 2003; Nadimi and Farpoor, 2013; Sarmast *et al*., 2017a). Carbonate and clay translocation occurred during periods with more humidity. Translocation of carbonates in deeper soil parts with more water available from the past resulted in the formation of calcic horizons. Clay illuviation due to the paucity of flocculation in the surface horizons facilitated the formation of argillic horizon in this geomorphic position (Khormali *et al*., 2003). On the other hand, translocated clay and carbonate were deposited during dryer periods. The repeated cycles of wetting and drying caused the formation of the above-mentioned morphological features. Coarse textured Ck horizon along with the adjacent Oligocene-Miocene calcareous marls caused the illuviation of calcium carbonate during more humid paleoclimate, in turn forming secondary calcium carbonate as pendants.

An Anhydritic Haplosalid (pedon 3) was formed on semi-stable mantled pediment (Fig. 2). High accumulation of anhydrite soft masses in this pedon is among the morphological characteristics observed in the field (Table 2, Fig. 2). Furthermore, high EC and SAR are plausible reasons for the formation of cemented salic horizon (Bznm) in the depths of this soil (Table 2, Fig. 2).

Pedon 4 located on the unstable surface of mantled pediment showed lithological discontinuity, gypsum pendants, and secondary calcium carbonate masses (Table 2, Fig. 2). Oligocene-Miocene calcareous marls and gypsiferous marls of Miocene age (Fig. 1) could be the only plausible sources for gypsum and calcite in this pedon. Formation of gypsic horizon between calcic horizons as a peculiar combination, is a proof for a polyphase soil genesis. The discontinuity observed in this pedon is another piece of evidence for soil climatic change through time. Micromorphological observations of desert varnish further support the above finding which will be discussed in the following sections. Morphological evidence showed that soils on stable and semi-stable mantled pediment were more developed in comparison to unstable mantled pediment. In their study of soils in Jiroft area, Sarmast *et al*. (2017a) reported that soil relative age indices of Feo/Fed and desert varnish cation ratio of (Ca+K)/Ti decreased with the increase in the stability of geomorphic surface, proving age increase in the mentioned trend.

Table 2. The selected morphological, physical, and chemical properties of the studied pedons

| Horizon | Depth (cm) | Morphological properties | | Physical properties | | | | Chemical properties | | | | | |
|---|---|---|---|---|---|---|---|---|---|---|---|---|---|
| | | Structure[a] | Concentrations[b] | Particle size distribution % | | | pH | EC | CCE[c] | Gy[d]+An[e] | Gy | An | SAR[f] |
| | | | | Sand | Silt | Clay | | dS m$^{-1}$ | % | % | % | % | (mmol L$^{-1}$)$^{0.5}$ |
| Pedon 1- Typic Calciargids- Stable surface of mantled pediment | | | | | | | | | | | | | |
| A | 0-5 | 1, m, abk | FDC, TOT | 59 | 26 | 15 | 7.7 | 0.6 | 11.00 | ng[g] | ng | ng | 0.8 |
| Btk | 5-40 | 1, m, abk | c, 2, I, CAM, MAT | 59 | 22 | 19 | 7.8 | 0.3 | 15.75 | ng | ng | ng | 0.8 |
| Crk | 40-100 | sg | c, 3, PE, CAX, BRF | 65 | 20 | 15 | 7.7 | 0.8 | 5.00 | ng | ng | ng | 1.6 |
| R | 100-150 | - | FDC, TOT | 79 | 12 | 9 | 7.8 | 0.6 | 4.25 | ng | ng | ng | 1.8 |
| Pedon 2- Typic Calciargids- Stable surface of mantled pediment | | | | | | | | | | | | | |
| A | 0-15 | 1, m, abk | FDC, TOT | 57 | 26 | 17 | 7.8 | 0.6 | 14.25 | ng | ng | ng | 0.8 |
| Btk1 | 15-40 | 1, m, abk | c, 2, I, CAM, MAT<br>f, 4, p, CBM, MAT | 43 | 32 | 25 | 7.7 | 1.0 | 17.75 | ng | ng | ng | 1.2 |
| Btk2 | 40-65 | 1, m, abk | c, 2, I, CAM, MAT<br>f, 4, p, CBM, MAT | 45 | 30 | 25 | 7.6 | 1.5 | 18.00 | ng | ng | ng | 1.8 |
| Btk3 | 65-90 | 1, m, abk | c, 2, I, CAM, MAT<br>f, 4, p, CBM, MAT | 55 | 20 | 25 | 7.8 | 0.5 | 19.75 | ng | ng | ng | 1.9 |
| Ck | 90-130 | sg | c, 3, PE, CAX, BRF | 83 | 10 | 7 | 8.1 | 0.4 | 10.50 | ng | ng | ng | 2.6 |
| R | 130-160 | - | FDC, TOT | 87 | 8 | 5 | 8.2 | 0.5 | 7.50 | ng | ng | ng | 1.9 |
| Pedon 3- Anhydritic Haplosalids- Semi-stable surface of mantled pediment | | | | | | | | | | | | | |
| Az | 0-8 | 1, m, abk | FDC, TOT<br>FDS, TOT | 45 | 36 | 19 | 7.4 | 16.5 | 15.25 | ng | ng | ng | 14.1 |
| Byzn1 | 8-30 | 1, m, abk | FDC, TOT<br>m, 3, I, GYM, MAT<br>FDS, TOT | 79 | 16 | 5 | 7.2 | 89.1 | 12.50 | 12.07 | 0.41 | 11.66 | 43.7 |
| Byzn2 | 30-52 | 1, m, abk | FDC, TOT<br>m, 3, I, GYM, MAT<br>FDS, TOT | 83 | 10 | 7 | 6.6 | 81.2 | 8.75 | 6.95 | 0.24 | 6.71 | 34.5 |
| Bzn | 52-75 | 1, m, abk | FDC, TOT<br>m, 3, I, GYM, MAT<br>FDS, TOT | 87 | 6 | 7 | 6.9 | 51.3 | 8.25 | 0.96 | 0.03 | 0.93 | 18.2 |
| Bznm1 | 75-100 | m | FDC, TOT<br>FDS, TOT | 83 | 8 | 9 | 6.8 | 66.8 | 7.00 | ng | ng | ng | 26.4 |
| Bznm2 | 100-140 | m | FDC, TOT<br>FDS, TOT | 81 | 8 | 11 | 7.0 | 54.4 | 7.00 | ng | ng | ng | 28.3 |
| Pedon 4- Typic Calcigypsids- Unstable surface of mantled pediment | | | | | | | | | | | | | |
| A | 0-10 | 1, m, abk | FDC, TOT | 45 | 34 | 21 | 7.6 | 0.8 | 17.50 | ng | ng | ng | 1.3 |
| Bk | 10-40 | 1, m, abk | c, 2, I, CAM, MAT | 37 | 46 | 17 | 7.2 | 5.9 | 14.25 | ng | ng | ng | 4.8 |
| By | 40-70 | sg | FDC, TOT<br>c, 2, PE, GYX, BRF | 81 | 14 | 5 | 7.4 | 7.0 | 6.25 | 6.61 | 6.61 | ng | 5.7 |
| 2Bk1 | 70-100 | 1, m, abk | c, 2, I, CAM, MAT | 71 | 14 | 15 | 7.3 | 10.3 | 14.75 | 0.08 | 0.08 | ng | 10.0 |
| 2Bk2 | 100-130 | 1, m, abk | c, 2, I, CAM, MAT | 69 | 16 | 15 | 7.4 | 6.9 | 19.00 | ng | ng | ng | 8.0 |
| 2C | 130-160 | sg | FDC, TOT | 81 | 14 | 5 | 7.5 | 7.0 | 10.25 | ng | ng | ng | 12.9 |
| Pedon 5- Typic Torrifluvents- Apex of alluvial fan | | | | | | | | | | | | | |
| A | 0-10 | 1, m, abk | FDC, TOT | 45 | 40 | 15 | 8.0 | 0.9 | 9 | ng | ng | ng | 1.52 |

| | | | | | | | | | | | | | |
|---|---|---|---|---|---|---|---|---|---|---|---|---|---|
| C | 10-140 | sg | FDC, TOT | 93 | 2 | 5 | 8.1 | 0.7 | 2 | ng | ng | ng | 1.64 |
| Pedon 6- Typic Torrifluvents- Stable surface of mid alluvial fan | | | | | | | | | | | | | |
| A | 0-10 | 1, m, abk | FDC, TOT | 45 | 36 | 19 | 8.0 | 0.6 | 15.75 | ng | ng | ng | 0.9 |
| C1 | 10-40 | sg | FDC, TOT | 83 | 12 | 5 | 7.7 | 0.4 | 5.50 | ng | ng | ng | 1.1 |
| C2 | 40-70 | sg | FDC, TOT | 83 | 12 | 5 | 7.7 | 0.7 | 3.50 | ng | ng | ng | 1.5 |
| C3 | 70-140 | sg | FDC, TOT | 79 | 14 | 7 | 7.7 | 0.6 | 4.50 | ng | ng | ng | 1.3 |
| Pedon 7- Typic Torrifluvents- Unstable surface of mid alluvial fan | | | | | | | | | | | | | |
| A | 0-10 | 1, m, abk | FDC, TOT | 45 | 48 | 7 | 7.4 | 1.4 | 8.75 | ng | ng | ng | 1.54 |
| C | 10-140 | sg | FDC, TOT | 93 | 2 | 5 | 8.0 | 0.2 | 1.00 | ng | ng | ng | 0.64 |
| Pedon 8- Anhydritic Haplosalids- Alluvial plain | | | | | | | | | | | | | |
| A | 0-5 | 1, m, abk | FDC, TOT<br>FDS, TOT | 25 | 44 | 31 | 7.6 | 4.5 | 21.00 | ng | ng | ng | 6.7 |
| Bkzn | 5-25 | 1, m, abk | c, 2, I, CAM, MAT<br>m, 3, PE, GYM, BRF<br>FDS, TOT | 57 | 30 | 13 | 7.1 | 45.4 | 19.00 | 4.7 | 0.16 | 4.54 | 22.3 |
| Byzn | 25-65 | 1, m, abk | FDC, TOT<br>m, 3, PE, GYM, BRF<br>FDS, TOT | 65 | 30 | 5 | 7.1 | 47.0 | 13.50 | 15.8 | 0.54 | 15.26 | 14.9 |
| Byn | 65-105 | 1, m, abk | FDC, TOT<br>m, 3, PE, GYM, BRF<br>FDS, TOT | 81 | 14 | 5 | 7.4 | 26.4 | 7.50 | 13.4 | 0.45 | 12.95 | 16.0 |
| C | 105-145 | sg | FDC, TOT<br>FDS, TOT | 87 | 6 | 7 | 8.1 | 26.7 | 7.25 | 2.7 | 0.10 | 2.60 | 77.5 |

[a] Structure: grade (1- weak); size (m- medium); type (abk- angular blocky, sg- single grain, m- massive)
[b] Concentrations: quantity (f- few, c- common, m- many); size (1- fine, 2- medium, 3- coarse, 4- very coarse); shape (I- irregular, PE- pendular, P- platy); kind (FDC- finely disseminated carbonates, FDS- finely disseminated salts, CAM- carbonate masses, CBM- clay bodies, GYM- gypsum masses, CAX- calcite crystals, GYX- gypsum crystals); location (MAT- in the matrix (not associated with peds/pores), TOT- throughout, BRF- on bottom of rock fragments)
[c] CCE: calcium carbonate equivalent
[d] Gy: gypsum
[e] An: anhydrite
[f] SAR: sodium adsorption ratio
[g] ng: negligible

Undeveloped soils (pedons 5, 6, and 7) with the same horizons and classifications (Typic Torrifluvents) were formed on different geomorphic surfaces of alluvial fan (Figs. 1, 2). The poor soil development on alluvial fans in the study area could be ascribed to sediments with an igneous origin derived from Jebalbarez Mountains far from calcareous Oligocene-Miocene and gypsiferous Miocene marls. In the eastern part of the study area (Fig. 1), coalescent alluvial fan (bajada) could not be formed in the current arid climate. Accordingly, a paleoclimate with more available humidity cannot be overlooked. The climatic model of alluvial fan development showed that aggradation in alluvial fan occurred in more humid climates (Armstrong *et al*., 2010; DeLong *et al*., 2008; Fletcher *et al*., 2010). Laminated varnish observed in this landform is yet another proof for the climatic fluctuations which will be discussed in more details in the following sections. Sarmast *et al.* (2017a) also reported that the relative age index of Feo/Fed activity ratio in stable and unstable mid alluvial fan was lower than apex. This, in turn, shows the relative increase in soil development during the formation and evolution of alluvial fan from apex to mid surfaces. The same researchers further reported the falling trend of desert varnish cation ratio age index from the mid towards the apex of alluvial fan.

An Anhydritic Haplosalid (pedon 8) with A, Bkzn, Byzn, Byn, and C horizons (Fig. 2) were formed on the alluvial plain. Calcic, anhydritic, and salic diagnostic horizons were formed in soils of this landform. During field studies, we investigated irregular carbonate masses in soil matrix and coarse anhydrite pendants beneath the rock fragments (Table 2, Fig. 2). Later stages of evaporation in host water during landform evolution were evidenced by high amounts of anhydrite in soils of alluvial plain. Besides, as the source of anhydrite, the adjacent Miocene gypsiferous marl could not be neglected.

### *3.2. Soil micromorphological characteristics*

Micromorphological investigations of pedons clearly showed the current arid conditions and the more humid paleoclimate in the history of the area (Table 3). Vesicular and platy microstructures along with calcitic crystallitic b-fabric observed in the A horizon of pedons 1 and 2 were also reported in several desert soils with yermic property (Gerasimova and Lebedeva-Verba, 2010).

#### *3.2.1. Calcite pedofeatures*

Calcite nodules, coatings, quasicoatings, and infillings, observed in the studied soils (Table 3), are among the most common pedofeatures recorded in the soils of arid and semi-arid areas (Durand *et al*., 2010). Various calcitic pedofeatures evidence certain environmental conditions, including dissolution, migration, and sedimentation processes which existed during their formation. Type and morphology of calcitic pedofeatures are mainly characterized by soil moisture and temperature regimes (Khormali *et al*., 2006). Illuviation of calcium carbonate from surface horizons occurring in arid and semi-arid environments with more available humidity, followed by reduced environmental moisture, caused the sedimentation of illuviated $CaCO_3$ in the groundmass and around soil grains and pores (Ayoubi *et al*., 2006; Bayat *et al*., 2017; Khormali *et al*., 2006).

The formation of orthic calcite nodule (Figs. 4a, b) was caused by the dissolution/recrystallization of calcite in the groundmass. The diffused gradual boundary of nodules is a proof for the in situ formation. Weak impregnation in certain parts of the groundmass induced by concentrated calcite microcrystals formed impregnated calcite nodules. The size of the nodules increased with the increase in the concentrated calcite crystals. Formation and morphology of calcite nodules were reported to be controlled by several processes such as dissolution/recrystallization, salt accumulation, hydromorphism (Sehgal and Stoops, 1972), soil texture (Wieder and Yaalon, 1982), soil stability (lack of erosion and vertic properties), and rapid sedimentation of carbonates due to continuous drying or $CO_2$ removal from soil solution (Sobecki and Wilding, 1983).

Recrystallization of illuviated calcium carbonate from surface horizons caused the formation of calcite coatings (Figs. 4c, d). The limpid color of the coatings proved that no impurities were associated with calcium carbonate and that the coatings were formed, during arid periods, through physicochemical processes with limited biological activity (Durand *et al*., 2010). Formation of quasicoatings were also attributed to the probable partial dissolution of the coatings (Figs. 4e, f). Calcite infillings seem to be formed by the deposition of soluble calcite in the pore spaces in the arid conditions of the area (Figs. 4g, h).

*3.2.2. Gypsum ($CaSO_4.2H_2O$) pedofeatures*

As the most common sulfate mineral in the soils of arid and semi-arid areas, gypsum was investigated by the micromorphological observations of pedons 3 (semi-stable surface of mantled pediment) and 8 (alluvial plain). Occurrence of gypsum in soils of the study area revealed that local environmental conditions with low rainfall prohibited the leaching of this mineral. Nodules and infillings composed of interlocked plates of gypsum were the dominant forms in semi-stable surface of mantled pediment (Figs. 5a, b). Moreover, infillings composed of lenticular (Fig. 5c), vermiform (Fig. 5d), platy (Fig. 5e), and interlocked plates (Fig. 5e) were the dominant gypsum forms in the alluvial plain (Table 3). Gypsum precipitation from a single point with a probable polyphasic origin might form gypsum nodules. Additionally, dissolution-precipitation processes are able to produce nodules (Poch *et al*., 2010). Various shapes of gypsum crystals in the studied soils are associated with the over-time microenvironmental changes in the soil. Lenticular gypsum indicates the light texture, unlimited pore space, and high ionic impurity in pedon 8 (Amit and Yaalon, 1996; Ayoubi *et al*., 2006; Hashemi *et al*., 2011). However, Cody (1979) reported that slow

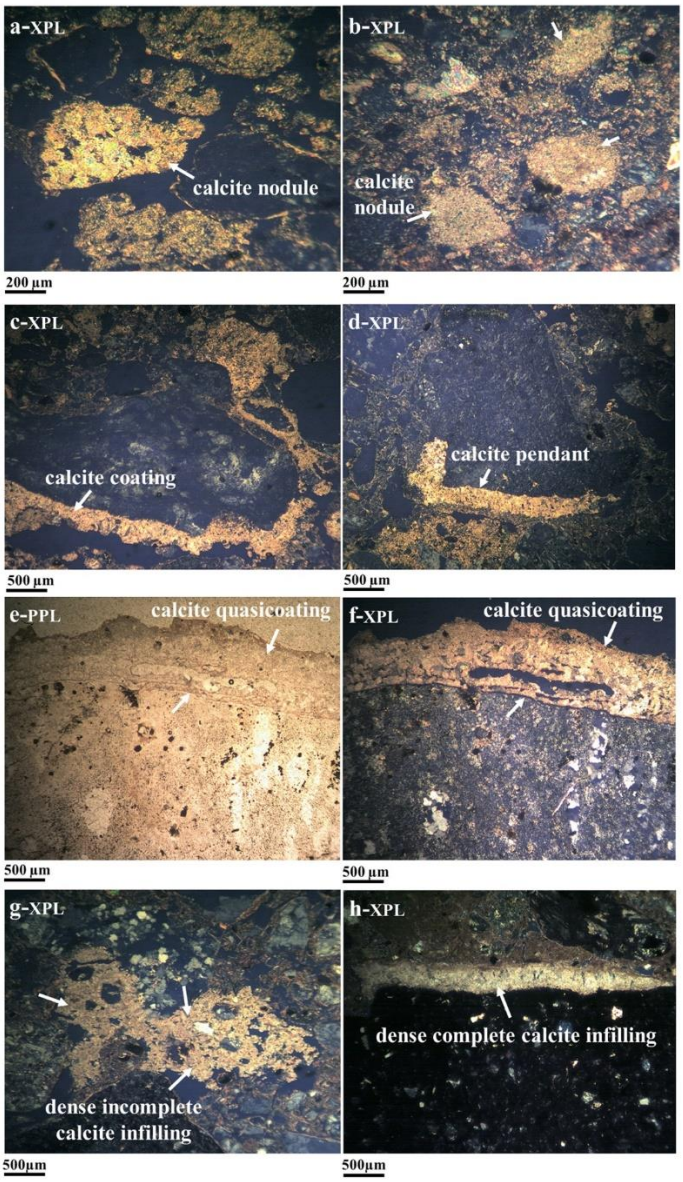


Fig. 4. Images of the calcite pedofeatures in the studied soils. Calcite nodule in Btk horizon, pedon 1 (a); Btk horizon, pedon 2 (b); calcite coating in Btk horizon, pedon 1(c); Btk horizon pedon 2 (d); calcite quasicoating in Btk horizon, pedon 1 (e, f); calcite infilling in Btk horizon, pedon 1 (g); Btk horizon, pedon 2 (h)

Table 3. Micromorphology description of the selected pedons

| Horizon | Depth (cm) | Microstructure | Groundmass | | | Pedofeatures |
|---|---|---|---|---|---|---|
| | | | c/f limit:10 µm | c/f related distribution | Micromass (b- fabric) | |
| Pedon 1- Typic Calciargids- Stable surface of mantled pediment | | | | | | |
| A | 0-5 | Subangular blocky<br>Vesicular | 2/8 | Open porphyric | Calcitic crystallitic<br>Granostriated | - |
| Btk | 5-40 | Subangular blocky | 2/8 | Chitonic | Calcitic crystallitic<br>Granostriated<br>Monostriated | Calcite orthic matrix nodules<br>Calcite coating<br>Calcite quasicoating<br>Calcite matrix infilling<br>Limpid clay coating<br>Layered clay coating<br>Lamella<br>Juxtaposed: clay coating with calcite infilling |
| Crk | 40-100 | Subangular blocky | 4/6 | Single spaced porphyric | Calcitic crystallitic<br>Granostriated | - |
| Pedon 2- Typic Calciargids- Stable surface of mantled pediment | | | | | | |
| A | 0-15 | Platy | 2/8 | Open porphyric | Calcitic crystallitic<br>Granostriated | - |
| Btk1 | 15-40 | Subangular blocky | 2/8 | Chitonic | Calcitic crystallitic<br>Granostriated | Calcite orthic matrix nodules<br>Calcite coating<br>Calcite quasicoating<br>Calcite matrix infilling<br>Limpid clay coating |
| Btk2 | 40-65 | Subangular blocky | 2/8 | Chitonic | Calcitic crystallitic<br>Granostriated | Calcite coating<br>Calcite pendant<br>Calcite quasicoating<br>Calcite matrix infilling<br>Limpid clay coating |
| Btk3 | 65-90 | Subangular blocky | 2/8 | Chitonic | Calcitic crystallitic<br>Granostriated | Calcite coating<br>Calcite quasicoating<br>Calcite matrix infilling<br>Limpid clay coating |
| Pedon 3- Anhydritic Haplosalids- Semi-stable surface of mantled pediment | | | | | | |
| Az | 0-8 | Subangular blocky<br>Vughs | 5/5 | Single spaced fine enaulic | Gypsitic/Anhydritic crystallitic<br>Granostriated | - |
| Byzn1 | 8-30 | Subangular blocky<br>Vughs | 5/5 | Single spaced porphyric | Gypsitic/Anhydritic crystallitic<br>Granostriated | Interlocked plates of gypsum crystals<br>Anhydrite crystals |
| Byzn2 | 30-52 | Subangular blocky<br>Vughs | 7/3 | Single spaced porphyric<br>Chitonic<br>Gefuric | Gypsitic/Anhydritic crystallitic<br>Granostriated | Halit coating<br>Calcite infilling<br>Interlocked plates of gypsum crystals<br>Anhydrite crystals |
| Bzn | 52-75 | Subangular blocky | 7/3 | Single spaced porphyric | Gypsitic/Anhydritic crystallitic | Limpid clay coating<br>Halit coating |

| | | | | | | |
|---|---|---|---|---|---|---|
| | | Vughs | | Chitonic<br>Gefuric | Granostriated | Calcite coating<br>Interlocked plates of gypsum crystals<br>Gypsum nodule<br>Anhydrite crystals<br>Limpid clay coating |
| Bznm1 | 75-100 | | | | | Halit coating<br>Calcite coating<br>Calcite infilling |
| | | Massive<br>Many vughs | 7/3 | Single spaced porphyric<br>Chitonic<br>Gefuric | Gypsitic/Anhydritic crystallitic<br>Granostriated | Interlocked plates of gypsum crystals<br>Anhydrite crystals<br>Anhydrite nodule<br>Limpid clay coating<br>Juxtaposed: anhydrite nodule with clay coating |
| Pedon 8- Anhydritic Haplosalids- Alluvial plain | | | | | | |
| Bkzn | 5-25 | Subangular blocky<br>Vughs | 1/9 | Double spaced porphyric | Calcitic crystallitic<br>Granostriated | Calcite coating<br>Gypsum crystals<br>Anhydrite crystals |
| Byzn | 25-65 | Subangular blocky<br>Vughs | 1/9 | Double spaced porphyric | Gypsitic/Anhydritic crystallitic<br>Granostriated | Lenticular gypsum crystals<br>Vermiform gypsum/anhydrite crystals<br>Interlocked plates of gypsum crystals |
| Byn | 65-105 | Subangular blocky<br>Vughs | 1/9 | Double spaced porphyric | Gypsitic/Anhydritic crystallitic<br>Granostriated<br>Speckled | Platy gypsum crystals<br>Platy anhydrite crystals<br>Interlocked plates of gypsum crystals<br>Interlocked plates of anhydrite crystals |

Crystallization of gypsum in alkaline conditions affected lenticular formation. On the other hand, Farpoor *et al*. (2003) reported reduced gravel and pore size, and finer textures as factors affecting lenticular gypsum formation. However, Jafarzadeh and Burnham (1992) and Toomanian *et al*. (2001) observed that lenticular crystals were the most dominant form of soil gypsum formed in a wide range of soil properties. Due to the high solubility of gypsum, a small variation in moisture content results in the solubility of lenticular crystals and formation of gypsum interlocked plates. Farpoor *et al*. (2003) concluded that the more available humidity of Pleistocene caused the dissolution of lenticular gypsum and formation of interlocked plates in 3Bym2 horizon of Rafsanjan area, central Iran. The massive structure in the depth of pedon 3 is ascribed to the high EC and SAR along with the interlocking of gypsum as plates in pore spaces (Table 2).

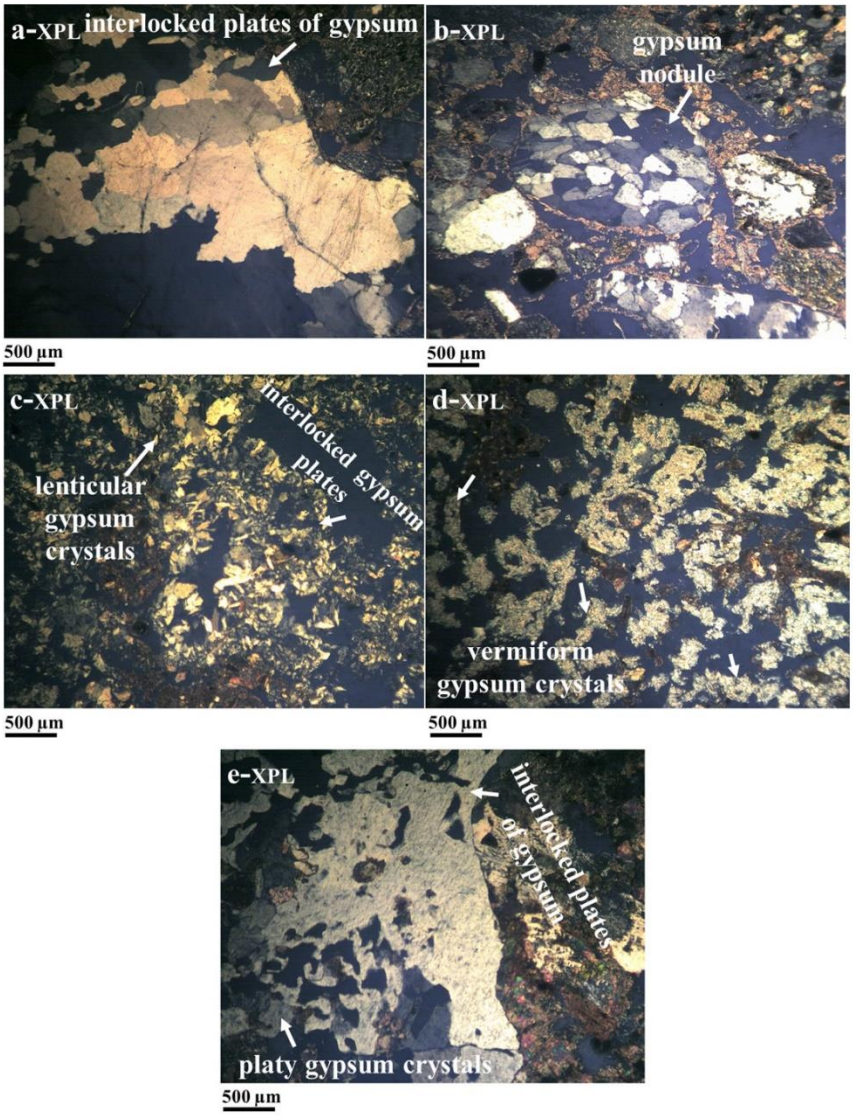


Fig. 5. Images of the gypsum pedofeatures in the studied soils. Interlocked plates of gypsum in Bzn horizon, pedon 3 (a); gypsum nodule in Bzn horizon, pedon 3 (b); lenticular gypsum in Byzn horizon, pedon 8 (c); vermiform gypsum in Byzn horizon pedon 8 (d); interlocked plates of gypsum in Byn horizon, pedon 8 (e).

### *3.2.3. Anhydrite ($CaSO_4$) pedofeatures*

Anhydrite occurred as pseudomorphs of gypsum crystals (Fig. 6) in pedons 3 (semi-stable surface of mantled pediment) and 8 (alluvial plain). These pseudomorphs indicated the transformation of gypsum into anhydrite. There exists a small amount of data on the transformation of gypsum into anhydrite in soil. Micromorphological observations in the present research revealed the formation and growth of anhydrite crystals after vermiforms and

interlocked plates of gypsum (Figs. 6a, b) as was also corroborated by Mees and Tursina (2010). Development of small randomly oriented and distributed anhydrite crystals inside gypsum crystals in pedon 3 (Fig. 6c) was attributed to the dehydration process (Aref, 2003). Butler (1970) further showed the transformation of gypsum into anhydrite through the dissolution/crystallization processes or dehydration (with or without basanite intermediate mineral formation). Furthermore, anhydrite crystals with a parallel orientation compared to gypsum crystals (Fig. 6d) showed repeated dehydration and hydration cycles (Dronkert, 1977; Mees and De Dapper, 2005).

In addition, typic anhydrite nodules were detected in Bznm1 horizon of pedon 3 (Figs. 6e, f). El-Tabakh *et al*. (2004) reported equidimensional or elongate anhydrite crystals as evidence for gypsum transformation into anhydrite. Anhydrite nodules were reported by El-Tabakh *et al*. (2004) and Wilson *et al*. (2013) in soils of Western Australia and Abu Dhabi, respectively.

### *3.2.4. Halite pedofeatures*

Halite evaporate mineral was found in the saline soils of the semi-stable surface of mantled pediment (Fig. 7). High soluble salts (EC of 16.5 to 89.1 dS $m^{-1}$) in pedon 3, caused by saline water evaporation, formed a coating of anhedral halite crystals around the grains (Fig. 7), in turn causing cementation and reducing infiltration in the soils of this geomorphic surface. Due to the hygroscopic habit of halite, the crystals would be partially dissoluble through water absorption. Thus, halite in soil mainly lacks a developed crystal face. In general, anhedral halite crystals flocculate soil grains and aggregate as a natural cementing agent (Mees and Tursina, 2010).

### *3.2.5. Clay pedofeatures*

Clay coatings with clear birefringence were observed around primary particles in the Btk horizons of pedons 1 and 2 (Figs. 8a, b, c). Formation of argillic horizon and clay coatings in the soils of arid and semi-arid environments (such as the area of the present research) with low SAR (Table 2) is an index of a paleoclimate with more available humidity in the past, further reported by many studies (Ayoubi *et al*., 2006; Bayat *et al*., 2017; Farpoor *et al*., 2012; Khormali *et al*., 2003;). The presence of more available humidity in the history of central Iran was also shown by Farpoor and Krouse (2008) who employed stable isotope geochemistry. More available humidity of the past caused carbonate removal from the soil surface followed by clay illuviation. The upcoming arid climate stopped the moisture front in the soil depth. Moreover, flocculation of illuviated clay by calcium carbonate led to the sedimentation of clay around primary particles and the formation of clay coatings (Bullock and Thompson, 1985).

Meanwhile, layered clay coatings (Fig. 8a) with clear sharp boundaries is a support for the presence of several illuviation processes or various illuviation rates with time. Changed soil/water suspension composition was further reported as a controlling factor in the formation of layered clay coatings. The composition of soil/water suspension was also changed through various stages of soil formation or weathering caused by illuviation in different parts of eluvial and illuvial horizons (Kühn *et al*., 2010; Theocharopoulos and Dalrymple, 1987). Extreme exposure of clay microlayers (lamella) with strong birefringence in the groundmass of pedon 1 is another proof of high stability in this geomorphic surface (Fig. 8c).

A special thick clay coating, common in sodic soils, was observed during the micromorphological observations of pedon 3 (Fig. 8d). Distribution and diffusion of clay particles by sodium ions (SAR=14.1-43.7 (mmol $L^{-1}$)$^{0.5}$) through the current arid climate in the semi-stable surface of mantled pediment are attributed to the formation of clay coatings compared to more available humidity of the past in pedons 1 and 2 (stable surface of mantled pediment) which were discussed earlier. Khormali *et al*. (2003) also found thick clay coatings in the saline and sodic soils of Fars Province. More thickness and absence of layering in the clay coatings of natric horizons compared to argillic horizons were further reported by Fedoroff and Courty (1987).

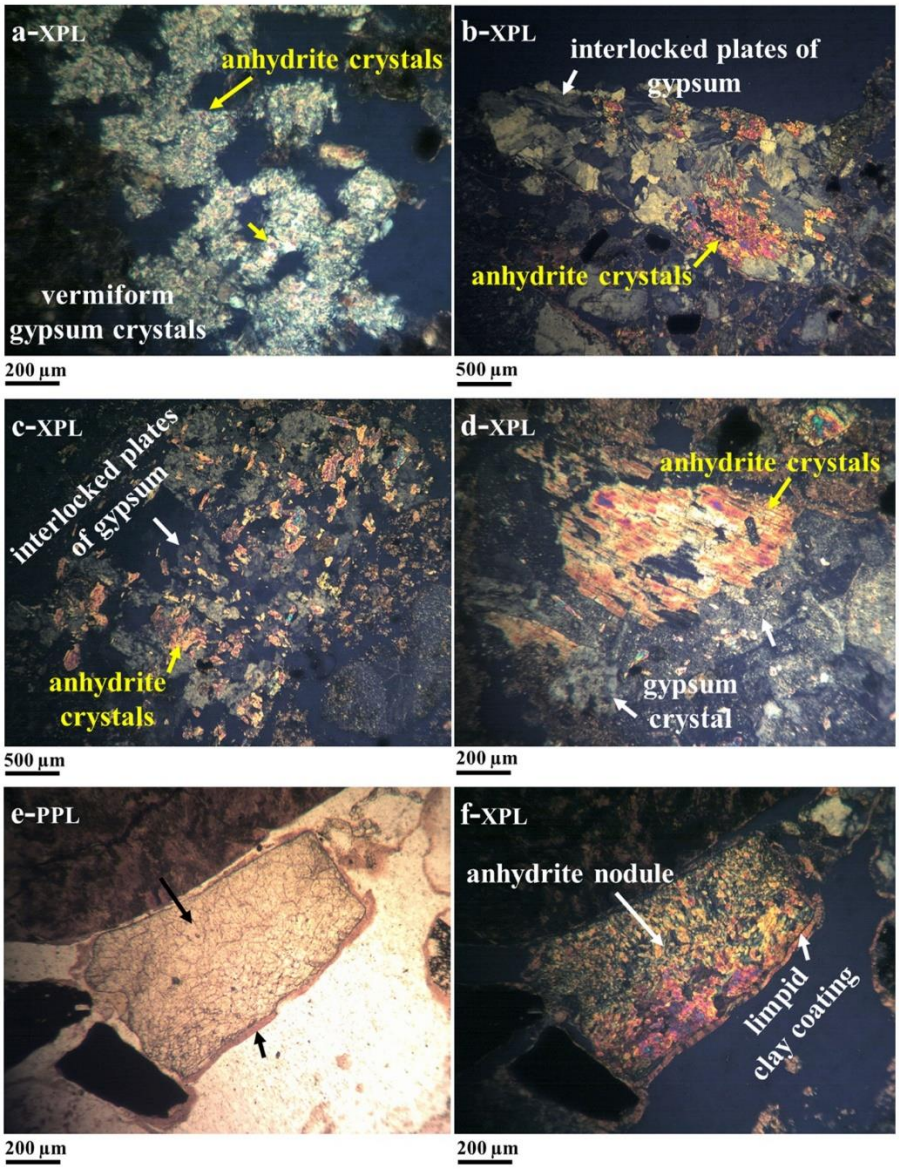


Fig. 6. Images of the anhydrite pedofeatures in studied soils. Growth of anhydrite crystals in vermiform gypsum in Byzn horizon, pedon 8 (a); growth of anhydrite crystals in interlocked plates of gypsum in Bznm1 horizon, pedon 3 (b); randomly anhydrite crystals in Byzn1 horizon, pedon 3 (c); gypsum and anhydrite crystals in Bzn horizon, pedon 3 (d); anhydrite nodule and juxtaposed anhydrite nodule-clay coating in Bznm1 horizon, pedon 3 (e, f)

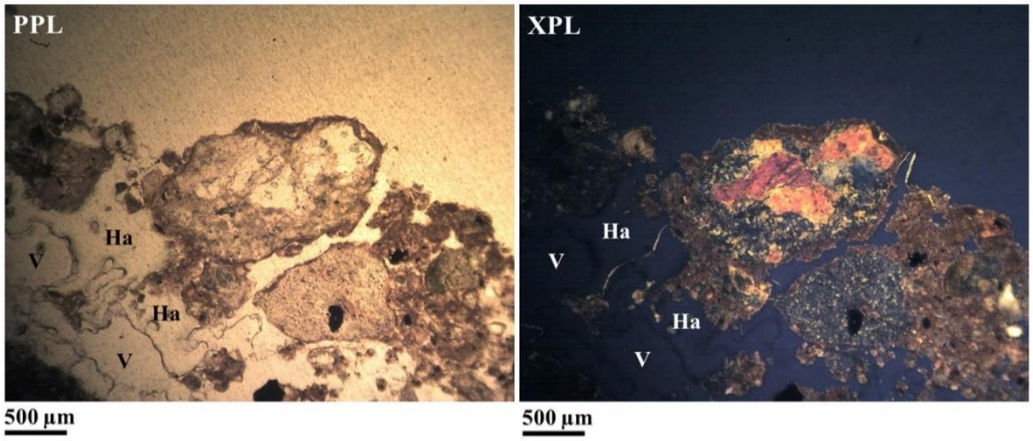


Fig. 7. Images of the halite pedofeatures in Byzn2 horizon, pedon 3 (Ha: halite; V: void)

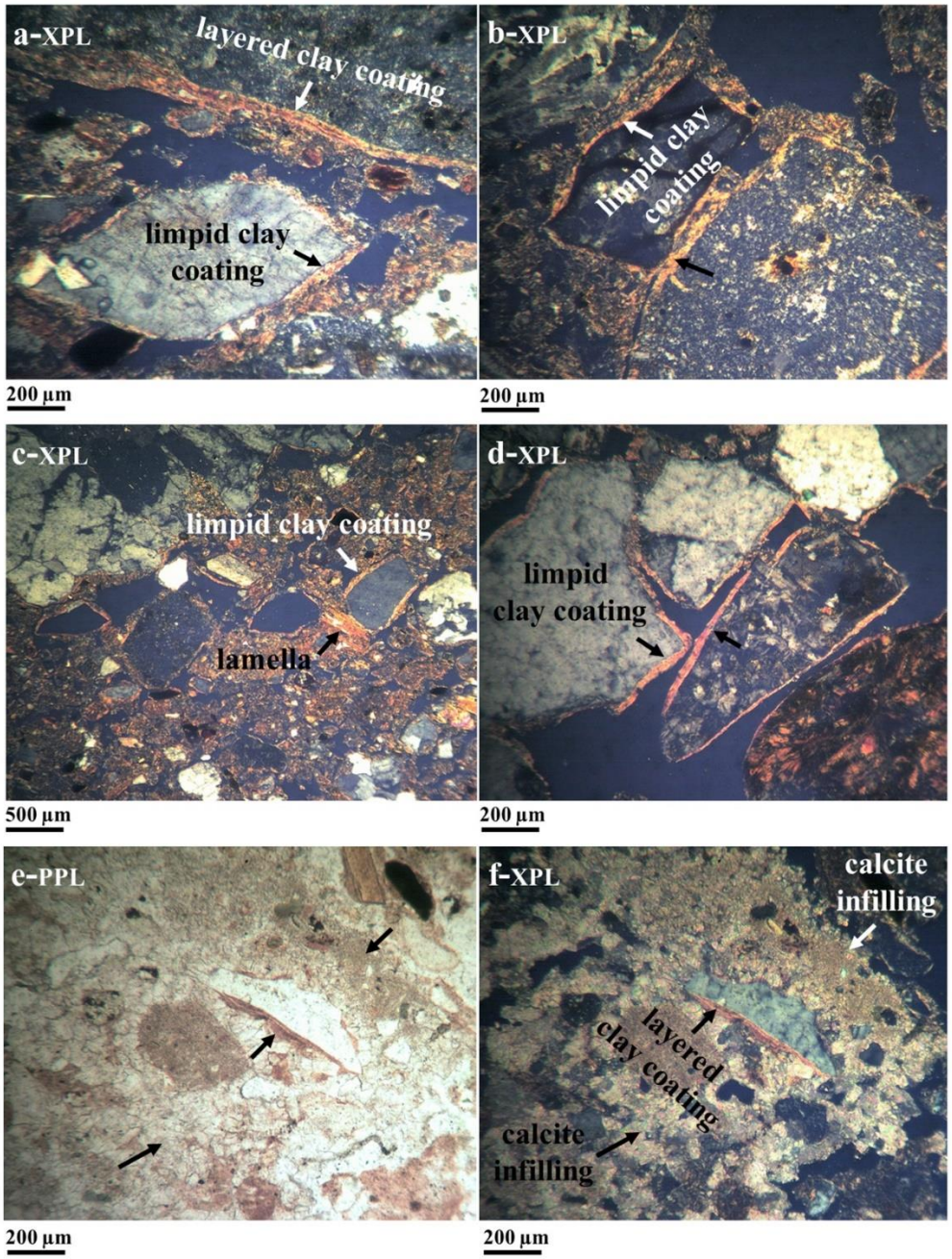


Fig. 8. Images of the clay pedofeatures in the studied soils. Clay coating in Btk horizon, pedon 1 (a, b); clay lamella in Btk horizon, pedon 1 (c); clay coating in Bznm1 horizon, pedon 3 (d); juxtaposed clay coating-calcite infilling in Btk horizon, pedon 1 (e, f)

*3.2.6. Compound pedofeatures*

Two compound pedofeatures were found in the thin sections of the studied soil. These pedofeatures characterized the temporal sequence of soil formation processes and paleoenvironmental conditions. The first pedofeature is the compound clay coating-calcite infilling (Figs. 9e, f) in Btk horizon of pedon 1, which is evidence of polygenesis. Clay coatings in this pedon were coated by calcite as infillings. Formation of this juxtaposed compound pedofeature is ascribed to the variation in local environmental conditions, proving that clay illuviation was followed by soil recalcification. Coating of calcite crystals on clay particles was caused by the more humid climate followed by an arid period, which formed a polygenetic soil. This was also confirmed by a study conducted in Isfahan, central Iran, using SEM investigations (Bayat *et al.*, 2017). Juxtaposed compound anhydrite nodule-clay coating pedofeature in Bznm1 horizon of pedon 3 is the second compound pedofeature (Figs. 6e, f), which is also

attributed to the environmental arid conditions of modern soils.

### *3.3. Climate change related to geological history*

The study area is an old shallow water body between the mountains affected by late Cretaceous to Miocene orogenic activities in central parts of Iran. Alluvial plain and semi-stable surface of mantled pediment were reported as the old lake and old lake periphery of Miocene age in the studied area, respectively (Sarmast *et al*., 2017a).

Calcite, gypsum, anhydrite, and halite were formed by the evaporation of saline intermountain water body, followed by warm and arid climatic conditions of Tertiary. The following trend could be highlighted for the micromorphological pedofeatures of pedons: calcite mineral was crystalized in the early stages of evaporation in the host water due to warm and arid climate of Tertiary. Removal of alkaline anions ($HCO_3^-$) following calcite crystallization created ideal conditions for the formation of gypsum. Increased salinity (followed by calcite and gypsum crystallization) and temperature during Quaternary, caused the formation of anhydrite in the later stages of evaporation. Anhydrite in the high temperature saline environment was formed by gypsum dehydration and remained stable (Wilson *et al*., 2013). Formation of anhydrite (together with gypsum) during marine water evaporation was also reported by El-Tabakh *et al*. (2004) and Melim and Scholle (2002) as the second common mineral caused by carbonate sedimentation.

### *3.4. Desert varnish*

#### *3.4.1. Optical properties of desert varnish*

The spaces in rock surface and between the minerals were filled by varnish, creating a soft surface on the rock (Fig. 9). Varnish thickness in the study area ranged 100-600 µm. Due to the microbasins and fissures in the rocks, varnish thickness was not uniform in all rocks. Varnish cover thickness was the lowest at the top of the grains and the highest on microbasins (Fig. 9).

Micromorphological observations indicated a difference in the color and texture of varnish compared to host rock (Fig. 10). Host rocks on stable and semi-stable mantled pediments, and unstable mid alluvial fan surface are cases where plagioclase microlites create a type of flowing texture; however, neither plagioclase nor flowing texture were found in the varnish cover. The color and texture differences between the varnish and the host rock made it possible to characterize the boundary between the varnish and the host rock. The distinctness and topography of the boundary between the varnish and the host rock in all studied geomorphic surfaces were abrupt and wavy, respectively. Potter and Rossman (1979, 1977) found a clearly different morphology between the varnish and host rock in the Nevada desert, with a distinct boundary. A sharp boundary between the varnish and its host rock was further reported by Jones (1991) in the coastal deserts of Northern Peru. Meanwhile, a distinct diffuse boundary with a wavy topography was found between the varnish and host rock boundary in Libyan Sahara desert (Zerboni, 2008).

A compositional contrast between the varnish and its host rock was clearly detected in petrography microscopic images (Fig. 11). The main components of desert varnish, including iron oxide spot, mottled opaque materials, and amorphous clay were also examined by micromorphological observations (Fig. 11). The combination of iron oxide-opaque grains, iron oxide-amorphous clay, and iron oxide-opaque grains-amorphous clay formed various colors depending on the combination type. The color of clay particles is an indicator of their purity. Light colored clays are pure whereas dark colored clays contain silt size or opaque impurities.

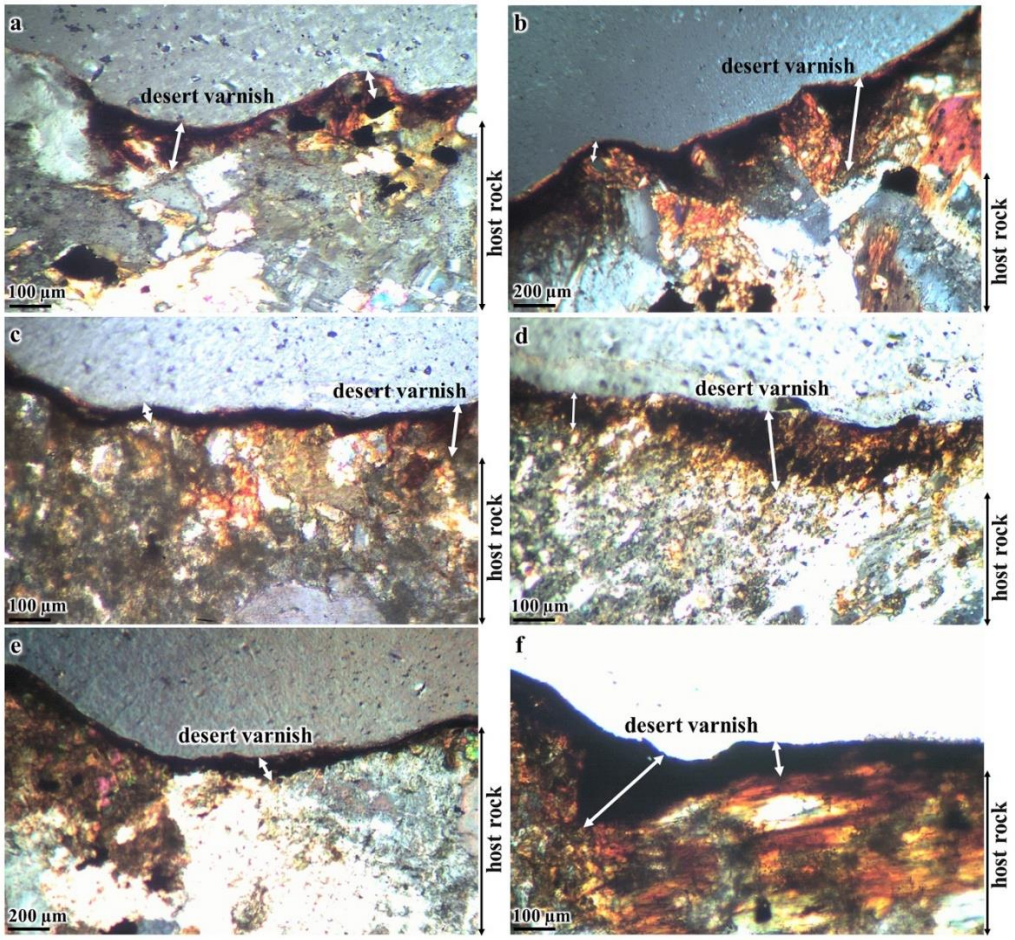


Fig. 9. Light microscope images of varnish ultrathin sections in different geomorphic surfaces representing the dark varnish smoothed the topography of the stone surface and microbasins were filled by varnish materials. Samples from the stable surface of mantled pediment (a), semi-stable surface of mantled pediment (b), unstable surface of mantled pediment (c), apex of alluvial fan (d), stable surface of mid alluvial fan (e), unstable surface of mid alluvial fan (f)

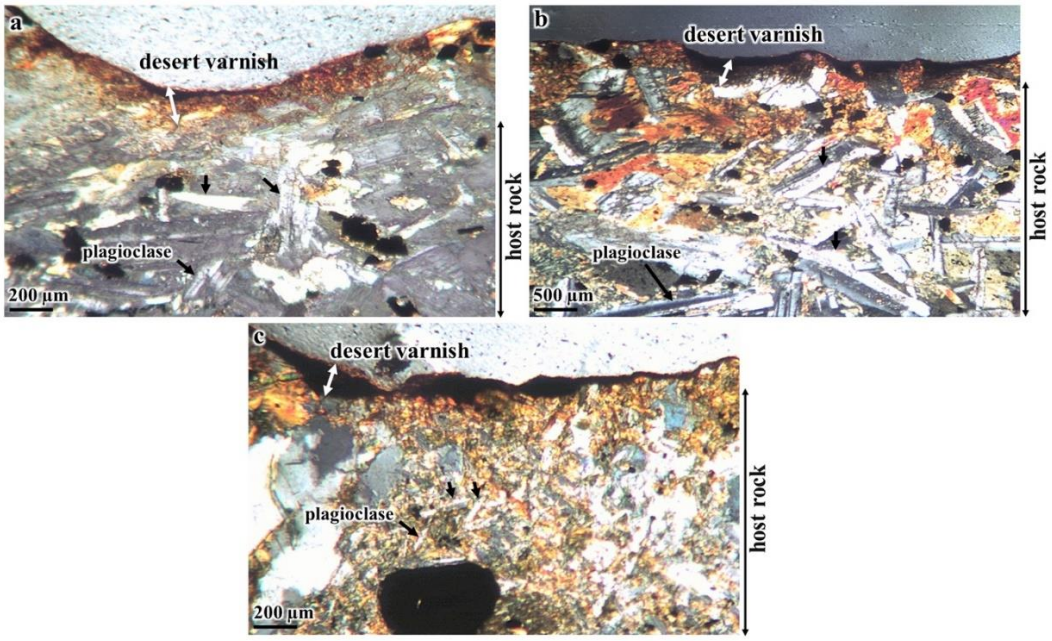


Fig. 10. Light microscope images of varnish ultrathin sections in stable (a) and semi-stable (b) surfaces of mantled pediment and unstable surface of mid alluvial fan (c), showing the morphology characteristics of desert varnish and the host rock

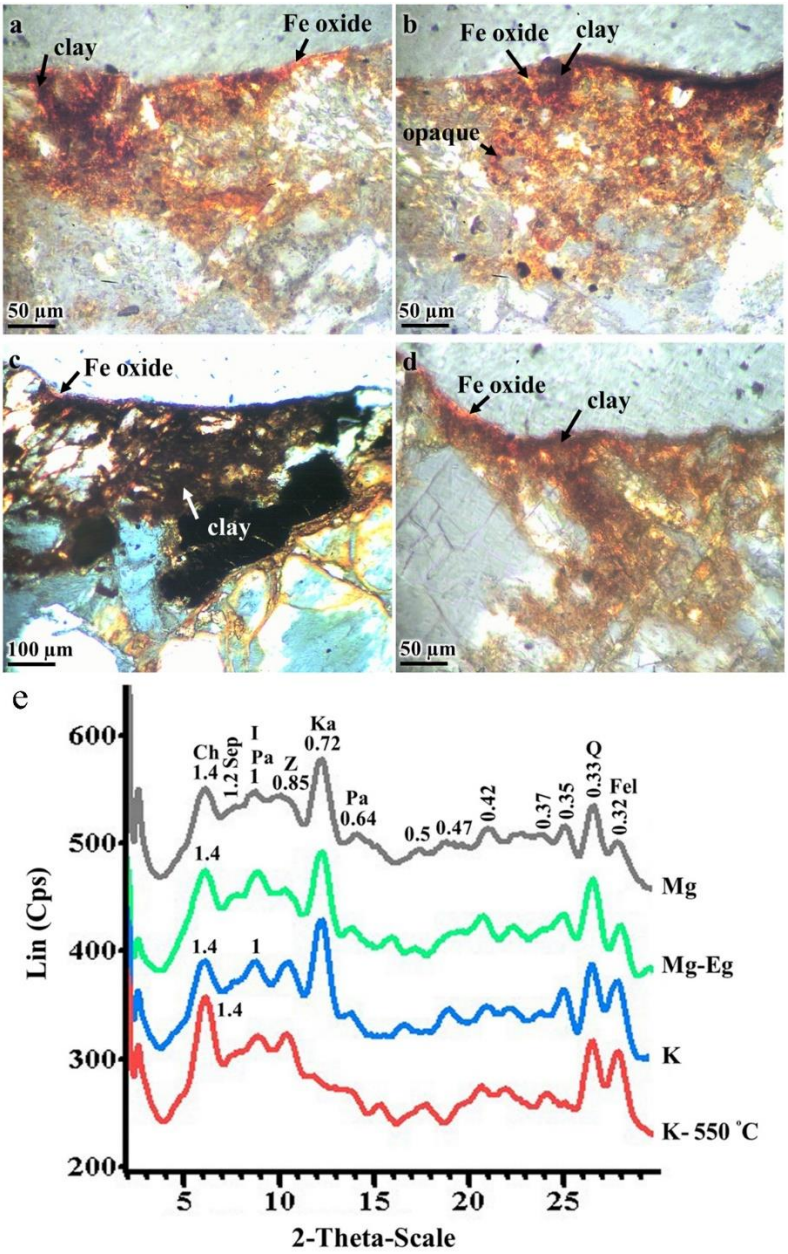


Fig. 11. Light microscope images of varnish ultrathin sections which show the desert varnish components. Samples from the stable surface of mantled pediment (a, b) and alluvial plain (c, d). As observed from the images, clay domains, Fe oxides, and opaque particles are the main components of desert varnish

*3.4.2. Environmental changes recorded in desert varnish*

*3.4.2.1. Crack varnish*

Crack varnish was found in unstable mantled pediment (Fig. 12a). As shown in Figure 12, crack varnish was filled up by varnish material and composed of orange and black layers. It seems that orange layers of crack varnish were formed when the rock crevices were open enough for illuviated clay particles to enter. As crevices continued opening, a black layer would be formed on the orange layer in the crevices (Liu and Dorn, 1996), creating a sequence of orange-black-orange layers in the rock crevices.

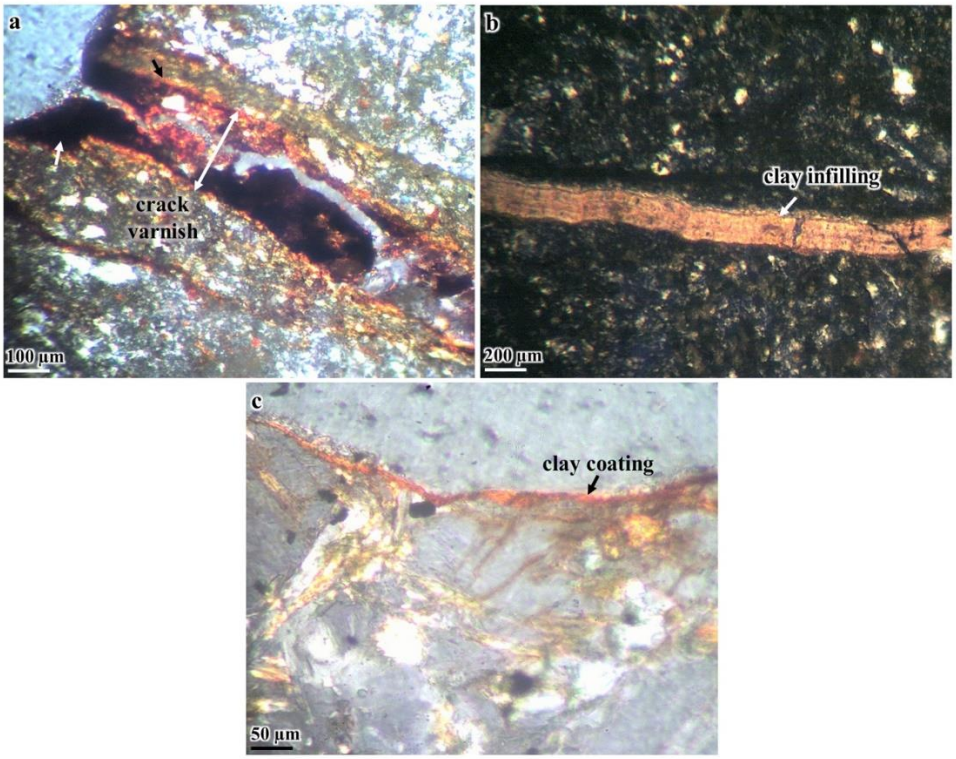


Fig. 12. Light microscope images of varnish ultrathin sections from the unstable surface of mantled pediment (a, b) and unstable surface of mid alluvial fan (b)

*3.4.2.2. Evidences of more humid paleoclimate*

Relatively pure infillings of clay with clear birefringence in the rock crevices on unstable mantled pediment surface were among the micromorphological features observed (Fig. 12b). Formation of clay infillings in the cracks proves the illuvial origin of the clay particles. Removal of flocculating agents is an important factor for clay illuviation (Scolt and Rabehorst, 1991). It seems that more humidity was required to leach the basic cations, calcium carbonate, and calcium sulfate from the soils of the area. Subsequently, clay suspension was illuviated into rock crevices.

Thee humidity of the current arid climate is not high enough for the development of such infillings; therefore, their formation could probably be ascribed to the more available humidity of the past environments. This was further supported by the soil data discussed in the previous sections. The same results were also reported by Zerboni (2008) regarding desert varnish in Messak Plateaus of Libian Sahara. Micromorphology observations of varnishes in that area showed internal microlayers of illuviated calcite and clay with strong birefringence which were attributed to more humid environmental conditions of early to mid-Holocene (5500-9200 uncal. YBP).

On the other hand, a thin coating of clay with weak birefringence was found on the rock surface of unstable mid alluvial fan (Fig. 12c). The thin coatings (dust film) are probably caused by the accumulation of clay particles originated from dust (aeolian sediments) during arid periods. The same results were also reported by Zerboni (2008) who concluded that coating was the upper microlayer of desert varnish mainly formed by the aeolian dust of last hyperarid millennia.

The above-mentioned results prove the presence of two different climates in the history of the area under study. In the period with more available humidity of the past, clay infillings were formed in rock crevices. The illuviated clay particles were preserved in the following less humid period, and clay coatings were also formed on rock surfaces. Zerboni (2008) also observed weak birefringent clay coatings formed on strong birefringent ones, indicating the climatic fluctuations from more humid to more arid environment.

*3.4.2.3. Internal structure of desert varnish*

Ultrathin sections of rocks with varnish cover showed two rubbly and laminated structures. Rubbly structure is a concentration of nanoparticles as light (yellow and orange) and

dark clusters with no coherent pattern of any sort (Garvie *et al*., 2008). On the other hand, laminated structure was comprised of nanoparticles concentrated in a pattern of high and dark laminae (Goldsmith *et al*., 2012).

Orange and dark microlaminations in desert varnishes were observed in the mantled pediment and alluvial fan geomorphic surfaces (Fig. 13a, b, c). The varnish formed on semi-stable mantled pediment further consisted of two orange and dark layers; however, no microlaminations were found (Fig. 13d). Formation of microlamination in the varnish revealed a variation in Mn, Fe, Al, and Si contents, in turn showing climatic fluctuation during time. Orange microlaminations are iron enriched and have been formed during arid periods, but black Mn-rich microlayers are proof of more humid periods (Liu, 2003; Liu and Broecker, 2013, 2008, 2007).

According to desert varnish formation models (Goldsmith *et al*., 2014; Jones, 1991; Thiagarajan and Lee, 2004), factors controlling Mn content in the varnish were climate dependent, and the amount of Mn in varnish decreased across arid climates. This was also supported by the chemical analyses of varnish microlamination by other researchers (Liu, 2003; Liu and Broecker, 2013, 2008, 2007). Microlamination analyses of varnishes in the area under study were also corroborated by the discussions presented in the previous sections concerning the climatic changes in the central parts of Iran. Orange microlayer in the upper part of varnish microlamination is a proof of the current arid climate. On the other hand, the frequency of orange and dark layers in the lower parts of microlamination proves the climatic fluctuations in the past environment of the study area.

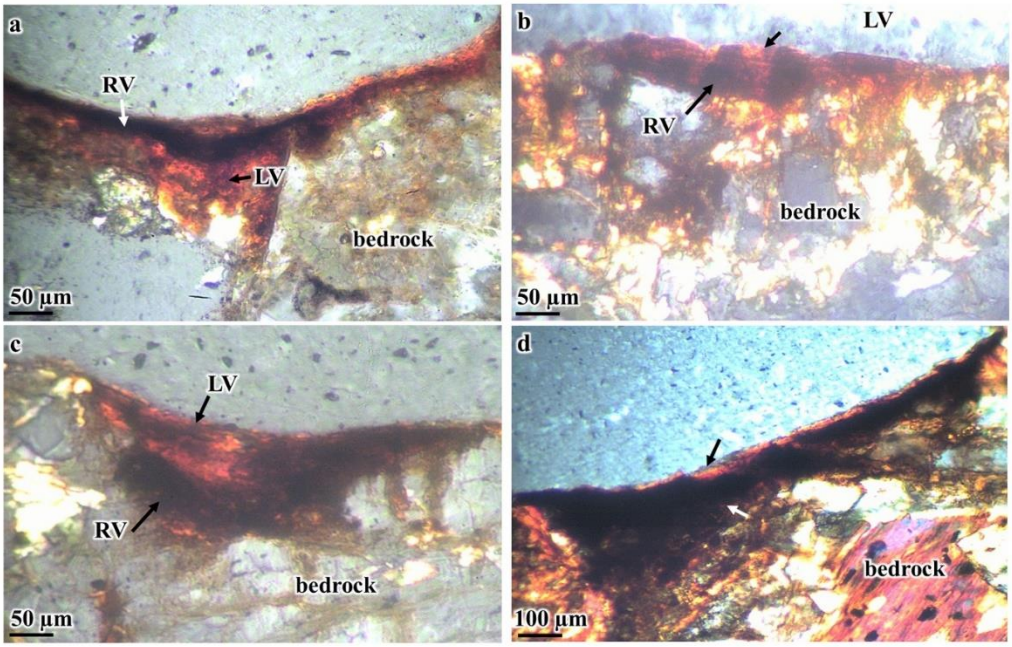


Fig. 13. Light microscope images of the selected varnish ultrathin sections belonging to the stable surface of mantled pediment (a), apex of alluvial fan (b), unstable surface of mid alluvial fan (c), semi-stable surface of mantled pediment (d). LV: laminated varnish. RV: rubbly varnish

## 4. Conclusions

Using micromorphology observations, we observed environmental and climatic fluctuations in the Central Iranian Plateau on undisturbed soil and desert varnish samples. Micromorphology records in soil and desert varnish showed a different climatic condition in the history of central Iran. Clay coatings and infillings in the thin sections of soils (with low SAR) and ultrathin sections of desert varnishes (rock crevices) were probably formed in a climate with more available moisture from the past. On the other hand, calcite, gypsum, anhydrite, and halite evaporites were formed in environmental conditions with less available humidity (arid to semi-arid). Furthermore, clay coatings in soils (with high SAR) and on the rock surfaces were formed during the arid periods while orange/dark microlamination of desert varnish was observed. Results of the present study clearly showed that micromorphology

investigations could be employed as a useful approach to identifying climatic and environmental variations in the Central Iranian Plateau.

**Acknowledgements**

The authors would like to express their special gratitude to Professor R.I. Dorn for his invaluable comments and recommendations in the preparation of the ultrathin section.

**References**

Amit, R., D.H. Yaalon, 1996. The micromorphology of gypsum and halite in reg soils-the Negev Desert, Israel. Earth Surface Processes and Landforms, 21 (12); 1127-1143.

Aref, M.A.M., 2003. Classification and depositional environments of Quaternary pedogenic gypsum crusts (gypcrete) from east of the Fayum Depression, Egypt. Sedimentary Geology, 155 (1); 87-108.

Armstrong, P.A., R. Perez, L.A. Owen, R.C. Finkel, 2010. Timing and controls on late Quaternary landscape development along the eastern Sierra El Mayor range front in northern Baja California, Mexico. Geomorphology, 114 (3); 415-430.

Artieda, O., J. Herrero, P.J. Drohan, 2006. Refinement of the differential water loss method for gypsum determination in soils. Soil Science Society of America Journal, 70 (6); 1932-1935.

Ayoubi, S., M.K. Eghbal, A. Jalalian, 2006. Study of micromorphological evidences of climate change during Quaternary recorded in paleosols from Isfahan. Journal of Water and Soil Science, 10 (1); 137-151.

Babakhani, A., N. Alavi Tehrani, M. Sabzehei, F. Ohanian, 1992. Geological map of Iran, Sabzevaran (1:250000). Geological Organization of Iran, Tehran.

Bayat, O., H. Karimzadeh, A. Karimi, M.K. Eghbal, H. Khademi, 2017. Paleoenvironment of geomorphic surfaces of an alluvial fan in the eastern Isfahan, Iran, in the light of micromorphology and clay mineralogy. Arabian Journal of Geosciences, 10 (4); 91-101.

Bullock, K.P., L. Thompson, 1985. Micromorphology of Alfisols. In: Douglas LA, editor. Soil micromorphology and soil classification. Madison, WI: Soil Science Society of America; p. 17-47.

Bullock, P., N. Fedoroff, A. Jongerius, G. Stoops, T. Tursina, U. Babel, 1985. Handbook for soil thin section description. Waine Research Publications, Wolverhampton, UK.

Butler, G.P., 1970. Holocene gypsum and anhydrite of the Abu Dhabi Sabkha, trucial coast: an alternative explanation of origin. In: Rau JL, Dellwig LF, editors. Proceedings of the third symposium on salt. Cleveland, Ohio: Northern Ohio Geological Society; p. 120-152.

Cody, R.D., 1979. Lenticular gypsum: occurrences in nature, and experimental determinations of effects of soluble green plant material on its formation. Journal of Sedimentary Petrology, 49 (3); 1015-1028.

Darvishzadeh, A., 1991. Geology of Iran. Neda Publication, Tehran.

DeLong, S.B., J.D. Pelletier, L.J. Arnold, 2008. Climate change triggered sedimentation and progressive tectonic uplift in a coupled piedmont-axial system: Cuyama Valley, California, USA. Earth Surface Processes and Landforms, 33 (7); 1033-1046.

Dorn, R.I., 2013. Rock coatings. In: Shroder J, Pope GA, editors. Treatise on geomorphology. San Diego, CA: Academic Press; p. 70-97.

Dorn, R.I., D.H. Krinsley, K.A. Langworthy, J. Ditto, T.J. Thompson, 2013. The influence of mineral detritus on rock varnish formation. Aeolian Research, 10; 61-76.

Dronkert, H., 1977. A preliminary note on a recent sabkha deposit in S. Spain. Revista del Instituto de Investigaciones Geológicas Diputación Provincial Universidad de Barcelona, 32; 153-166.

Durand, N., H.C. Monger, M.G. Canti, 2010. Calcium carbonate features. In: Stoops G, Marcelino V, Mees F, editors. Interpretation of micromorphological features of soils and regoliths. Amsterdam, Netherlands: Elsevier; p. 149-182.

El-Tabakh, M., A. Mory, B.C. Schreiber, R. Yasin, 2004. Anhydrite cements after dolomitization of shallow marine Silurian carbonates of the Gascoyne Platform, Southern Carnarvon Basin, Western Australia. Sedimentary Geology, 164 (1); 75-87.

Farpoor, M.H., M.K. Eghbal, H. Khademi, 2003. Genesis and micromorphology of saline and gypsiferous Aridisols on different geomorphic surfaces in Nough area, Rafsanjan. Journal of Water and Soil Science, 7 (3); 71-93.

Farpoor, M.H., M. Irannejad, 2013. Soil genesis and clay mineralogy on Aliabbas River alluvial fan, Kerman Province. Arabian Journal of Geosciences, 6 (3); 921-928.

Farpoor, M.H., H.R. Krouse, 2008. Stable isotope geochemistry of sulfur bearing minerals and clay mineralogy of some soils and sediments in Loot Desert, central Iran. Geoderma, 146 (1); 283-290.

Farpoor, M.H., M. Neyestani, M.K. Eghbal, I. Esfandiarpour Borujeni, 2012. Soil–geomorphology relationships in Sirjan playa, south central Iran. Geomorphology, 138 (1); 223-230.

Fedoroff, N., M.A. Courty, 1987. Morphology and distribution of textural features in arid and semiarid regions. In: Fedoroff N, Bresson LM, Courty MA, editors. Micromorphologie des sols, soil micromorphology. Paris, France: Association Française pour l'Etude du Sol (AFES); p. 213-219.

Fletcher, K.E.K., W.D. Sharp, K.J. Kendrick, W.M. Behr, K.W. Hudnut, T.C. Hanks, 2010. $^{230}$Th/U dating of a late Pleistocene alluvial fan along the southern San Andreas fault. Geological Society of America Bulletin, 122 (9-10); 1347-1359.

Gammon, N.J.R., 1951. Determination of total potassium and sodium in sandy soils by flame photometer. Soil Science, 71 (3); 211-214.

Garvie, L.A.J., D.M. Burt, P.R. Buseck, 2008. Nanometer-scale complexity, growth, and diagenesis in desert varnish. Geology, 36 (3); 215-218.

Gee, G.W., J.W. Bauder, 1986. Particle size analysis. In: Klute A, editor. Methods of soil analysis. Madison, WI: Soil Science Society of America; p. 388-409.

Gerasimova, M., M. Lebedeva-Verba, 2010. Topsoils-mollic, takyric, and yermic Horizons. In Stoops G,

Marcelino V, Mees F, editors. Interpretation of micromorphological features of soils and regolith. Amsterdam, Netherlands: Elsevier; p. 351-364.

Goldsmith, Y., Y. Enzel, M. Stein, 2012. Systematic Mn fluctuations in laminated rock varnish developed on coeval early Holocene flint artifacts along a climatic transect, Negev Desert, Israel. Quaternary Research, 78 (3); 474-485.

Goldsmith, Y., M. Stein, Y. Enzel, 2014. From dust to varnish: geochemical constraints on rock varnish formation in the Negev Desert, Israel. Geochimica et Cosmochimica Acta, 126; 97-111.

Gutiérrez, M., 2005. Climatic geomorphology. In Shroder J, editor. Developments in earth surface processes. Amsterdam, the Netherlands: Elsevier; p. 227-383.

Gunal, H., M.D. Ransom, 2006. Clay illuviation and calcium carbonate accumulation along a precipitation gradient in Kansas. Catena, 68 (1); 59-69.

Hashemi, S.S., M. Baghernejad, H. Khademi, 2011. Micromorphology of gypsum crystals in southern Iranian soils under different moisture regimes. Journal of Agricultural Science and Technology, 13; 273-288.

Hodge, V.F., D.E. Farmer, T. Diaz, R.L. Orndorff, 2005. Prompt detection of alpha particles from 210 Po: another clue to the origin of rock varnish? Journal of Environmental Radioactivity, 78 (3); 331-342.

Jafarzadeh, A.A., C.P. Burnham, 1992. Gypsum crystals in soils. European Journal of Soil Science, 43 (3); 409-420.

Jones, C.E., 1991. Characteristics and origin of rock varnish from the hyperarid coastal deserts of northern Peru. Quaternary Research, 35 (1); 116-129.

Kemp, R.A., 2013. Paleosols and wind-blown sediments/ soil micromorphology. Reference Module in Earth Systems and Environmental Sciences, 2; 381-391.

Khademi, H., A.R. Mermut, 2003. Micromorphology and classification of Argids and associated gypsiferous Aridisols from central Iran. Catena, 54 (3); 439-455.

Khormali, F., A. Abtahi, S. Mahmoodi, G. Stoops, 2003. Argillic horizon development in calcareous soils of arid and semiarid regions of southern Iran. Catena, 53 (3); 273-301.

Khormali, F., A. Abtahi, G. Stoops, 2006. Micromorphology of calcitic features in highly calcareous soils of Fars Province, Southern Iran. Geoderma, 132 (1); 31-46.

Khormali, F., M. Ajami, 2011. Pedogenetic investigation of soil degradation on a deforested loess hillslope of Golestan Province, Northern Iran. Geoderma, 167; 274-283.

Krinsley, D.B., 1970. A geomorphological and paleoclimatological study of the playas of Iran. Geological Survey, United States Department of Interior, Washington DC.

Kühn, P., J. Aguilar, R. Miedema, 2010. Textural pedofeatures and related horizons. In Stoops G, Marcelino V, Mees F, editors. Interpretation of micromorphological features of soils and regolith. Amsterdam, Netherlands: Elsevier; p. 217-240.

Liu, T., 2003. Blind testing of rock varnish microstratigraphy as a chronometric indicator: results on late Quaternary lava flows in the Mojave Desert, California. Geomorphology, 53 (3); 209-234.

Liu, T., W.S. Broecker, 2000. How fast does rock varnish grow? Geology, 28 (2); 183-186.

Liu, T., W.S. Broecker, 2007. Holocene rock varnish microstratigraphy and its chronometric application in the drylands of western USA. Geomorphology, 84 (1); 1-21.

Liu, T., W.S. Broecker, 2008. Rock varnish microlamination dating of late Quaternary geomorphic features in the drylands of western USA. Geomorphology, 93 (3); 501-523.

Liu, T., W.S. Broecker, 2013. Millennial-scale varnish microlamination dating of late Pleistocene geomorphic features in the drylands of western USA. Geomorphology, 187; 38-60.

Liu, T., R.I. Dorn, 1996. Understanding the spatial variability of environmental change in drylands with rock varnish microlaminations. Annals of the Association of American Geographers, 86 (2); 187-212.

Mees, F., M. De Dapper, 2005. Vertical variations in basanite distribution patterns in near-surface sediments, southern Egypt. Sedimentary Geology, 181 (3); 225-229.

Mees, F., T.V. Tursina, 2010. Salt minerals in saline soils and salt crusts. In Stoops G, Marcelino V, Mees F, editors. Interpretation of micromorphological features of soils and regolith. Amsterdam, Netherlands: Elsevier; p. 441-461.

Melim, L.A., P.A. Scholle, 2002. Dolomitization of the capitan formation for reef facies (Permian, west Texas and New Mexico): Seepage reflux revisited. Sedimentology, 49 (6); 1207-1227.

Moazallahi, M., M.H. Farpoor, 2009. Soil micromorphology and genesis along a climotoposequence in Kerman Province, Central Iran. Australian Journal of Basic and Applied Sciences, 3 (4); 4078-4084.

Murphy, C.P., 1986. Thin section preparation of soils and sediments. AB Academic Publishers, Berkhamsted, Herts, UK.

Nadimi, M., M.H. Farpoor, 2013. Genesis and clay mineralogy of soils on different geomorphic surfaces in Mahan-Joupar area, Central Iran. Arabian Journal of Geosciences, 6 (3); 825-833.

Nelson, R.E., 1982. Carbonate and gypsum. In Page AL, editor. Methods of soil analysis. Madison, WI: Soil Science Society of America; p. 181-196.

Perry, R.S., J.B. Adams, 1978. Desert varnish: evidence for cyclic deposition of manganese. Nature, 276 (5687); 489-491.

Poch, R.M., O. Artieda, J. Herrero, M. Lebedeva-Verba, 2010. Gypsic features. In Stoops G, Marcelino V, Mees F, editors. Interpretation of micromorphological features of soils and regolith. Amsterdam, Netherlands: Elsevier; p. 195-216.

Potter, R.M., G.R. Rossman, 1977. Desert varnish: the importance of clay minerals. Science, 196 (4297); 1446-1448.

Potter, R.M., G.R. Rossman, 1979. The manganese and iron-oxide mineralogy of desert varnish. Chemical Geology, 25 (1–2); 79-94.

Ringbom, A., G. Pensar, E. Wänninen, 1958. A complexometric titration method for determining calcium in the presence of magnesium. Analytica Chimica Acta, 19; 525-531.

Sarmast, M., M.H. Farpoor, I. Esfandiarpour Boroujeni, 2016. Comparing Soil Taxonomy (2014) and

updated WRB (2015) for describing calcareous and gypsiferous soils, Central Iran. Catena, 145; 83-91.

Sarmast, M., M.H. Farpoor, I. Esfandiarpour Boroujeni, 2017a. Soil and desert varnish development as indicators of landform evolution in Central Iranian deserts. Catena, 149; 98-109.

Sarmast, M., M.H. Farpoor, I. Esfandiarpour Boroujeni, 2017b. Magnetic susceptibility of soils along a lithotoposequence in southeast Iran. Catena, 156; 252-262.

Schoeneberger, P.J., D.A. Wysocki, E.C. Benham, Soil Survey Staff, 2012. Field book for describing and sampling soils. Natural Resources Conservation Service. National Soil Survey Center, Lincoln, NE.

Scolt, M.H., M.C. Rabenhorst, 1991. Micromorphology of argillic horizons in an upland/tidal marsh catena. Soil Science Society of America Journal, 55; 443-450.

Sehgal, J.L., G. Stoops, 1972. Pedogenic calcite accumulation in arid and semiarid regions of the Indo-Gangetic alluvial plain of erstwhile Punjab (India) - Their morphology and origin. Geoderma, 8 (1); 59-72.

Sengör, A.M.C., D. Altiner, A. Cin, T. Ustaömer, K.J. Hsü, 1988. Origin and assembly of the Tethyside orogenic collage at the expense of Gondwana land. Geological Society, 37 (1); 119-181.

Sobecki, T.M., L.P. Wilding, 1983. Formation of calcic and argillic horizons in selected soils of the Texas Coast Prairie. Soil Science Society of America Journal, 47 (4); 707-715.

Stoops, G., 2003. Guidelines for analysis and description of soil and regolith thin sections. Soil Science Society of America, Madison, Wisconsin.

Stoops, G., 2010. Micromorphology as a tool in soil and regolith studies. In Stoops G, Marcelino V, Mees F, editors. Interpretation of micromorphological features of soils and regolith. Amsterdam, Netherlands: Elsevier; p. 1-13.

Theocharopoulos, S.P., J.B. Dalrymple, 1987. Experimental construction of illuviation cutans (channel Argillans) with differing morphological and optical properties. In: Fedoroff N, Bresson LM, Courty MA, editors. Micromorphologie des sols, soil micromorphology. Paris, France: Association Française pour l'Etude du Sol (AFES); p. 245-250.

Thiagarajan, N., C.T.A. Lee, 2004. Trace-element evidence for the origin of desert varnish by direct aqueous atmospheric deposition. Earth and Planetary Science Letters, 224 (1); 131-141.

Toomanian, N., A. Jalalian, M.K. Eghbal, 2001. Genesis of gypsum enriched soils in north-west Isfahan, Iran. Geoderma, 99 (3); 199-224.

Van Wambeke, A., 1986. Newhall simulation model, a basic program for the IBM PC [floppy disk computer file]. Department of Agronomy, Cornell University, Ithaca, New York, USA.

Watchman, A., 2000. A review of the history of dating rock varnishes. Earth-Science Reviews, 49 (1); 261-277.

Wieder, M., D.H. Yaalon, 1982. Micromorphological fabrics and developmental stages of carbonate nodular forms related to soil characteristics. Geoderma, 28 (3-4); 203-220.

Wilson, M.A., S.A. Shahid, M.A. Abdelfattah, J.A. Kelley, J.E. Thomas, 2013. Anhydrite formation on the Coastal Sabkha of Abu Dhabi, United Arab Emirates. In: Shahid SA, Taha FK, Abdelfattah MA, editors. Developments in soil classification, land use planning and policy implications: innovative thinking of soil inventory for land use planning and management of land resources. Netherlands: Springer SBM Publishing; p. 175-201.

Zachos, J.C., K.C. Lohmann, J.C. Walker, S.W. Wise, 1993. Abrupt climate change and transient climates during the paleogene: a marine perspective. Journal of Geology, 101 (2); 191–213.

Zerboni, A., 2008. Holocene rock varnish on the Messak plateau (Libyan Sahara): chronology of weathering processes. Geomorphology, 102 (3); 640-65.